Available online at www.sciencedirect.com
SCIENCE DIRECT®
Marine Geology 205 (2004) 185–206
MARINE GEOLOGY
INTERNATIONAL JOURNAL OF MARINE GEOLOGY, GEOCHEMISTRY AND GEOPHYSICS
www.elsevier.com/locate/margeo

Neogene history of the Deep Western Boundary Current at Rekohu sediment drift, Southwest Pacific (ODP Site 1124)

Leah H. Joseph *, David K. Rea, Ben A. van der Pluijm

Department of Geological Sciences, University of Michigan, Ann Arbor, MI 48109-1063, USA

Received 25 January 2002; received in revised form 18 July 2003; accepted 26 January 2004

Abstract

ODP Site 1124, located 600 km east of the North Island of New Zealand, records post-middle Oligocene variations in the Pacific Deep Western Boundary Current (DWBC) and New Zealand's climatic and tectonic evolution. Sediment parameters, such as terrigenous grain size, flux, magnetic fabric, and non-depositional episodes, are used to interpret DWBC intensity and Antarctic climate. Interpretations of DWBC velocities indicate that the Antarctic Circumpolar Current reached modern intensities at ~23 Ma, as the tectonic seaways expanded, completing the thermal isolation of Antarctica. Periods of more intense bottom water formation are suggested by the presence of hiatuses formed under the DWBC at 22.5–17.6, 16.5–15, and 14–11 Ma. The oldest interval of high current intensity occurs within a climatically warm period during which the intensity of thermohaline circulation around Antarctica increased as a result of recent opening of circum-Antarctic gateways. The younger hiatuses represent glacial periods on Antarctica and major fluctuations in the East Antarctic Ice Sheet, whereas intervals around the hiatuses represent times of relative warmth, but with continued current activity. The period between 11 to 9 Ma is characterized by conditions surrounding a high velocity DWBC around the time of the formation and stabilization of the West Antarctic Ice Sheet. The increased terrigenous input may result from either changing Antarctic conditions or more direct sediment transport from New Zealand. The Pacific DWBC did not exert a major influence on sedimentation at Site 1124 from 9 Ma to the present; the late Miocene to Pleistocene sequence is more influenced by the climatic and tectonic history of New Zealand. Despite the apparent potential for increased sediment supply to this site from changes in sediment channeling, increasing rates of mountain uplift, and volcanic activity, terrigenous fluxes remain low and constant throughout this younger period.
© 2004 Elsevier B.V. All rights reserved.

Keywords: paleoclimate; Southwest Pacific Deep Western Boundary Current; Antarctic Circumpolar Current; ocean gateways; ODP Site 1124; grain size and magnetic fabric analysis

1. Introduction

The Southern Ocean, and its surface and deep circulation, are critical components of the conveyor system of heat transport of the world's oceans. The Southern Ocean allows for interconnection between the world's oceans and the mixing of

* Corresponding author. Present address: Environmental Studies Program, Department of Geoscience, Hobart and William Smith Colleges, Geneva, NY 14456, USA.
Tel.: +1-(315)-781-3954; Fax: +1-(315)-781-3860.
E-mail addresses: ljoseph@hws.edu (L.H. Joseph), davidrea@umich.edu (D.K. Rea), vdpluijm@umich.edu (B.A. van der Pluijm).

0025-3227/04/$ – see front matter © 2004 Elsevier B.V. All rights reserved.
doi:10.1016/S0025-3227(04)00023-4

water masses within the Antarctic Circumpolar Current (ACC). In addition, cold waters that form, sink off the Antarctic margin and mix in this zone, become the bottom waters of the world, upwelling to the surface elsewhere. This transport system of water and properties of the individual water masses link the polar regions to the global climate system as an integral part in the regulation of Earth's climatic regime (Broecker, 1997; Orsi et al., 1999).

This study investigates the Southwest Pacific Deep Western Boundary Current (DWBC) off the eastern coast of New Zealand through the study of sedimentary characteristics obtained from the late Oligocene through Pleistocene sediment of the Rekohu sediment drift (ODP Site 1124). Variation in the velocity of this DWBC may have implications for the development and fluctuation of the ACC to modern intensities, as the intensity of DWBC flow is likely modulated by the strength of ACC circulation, as well as climatic conditions, ice sheet coverage and stability and the presence of sea ice (i.e. Keller and Barron, 1983; Carter et al., 1996). Characteristics such as grain alignment and grain size allow interpretations of the bottom current intensities that can reflect global climate conditions.

2. Background

2.1. Antarctic Bottom Water and the Southwest Pacific DBWC

Waters upwell and/or diffuse globally from the deep sea as part of oceanic thermohaline circulation in several locations and are often broad and diffuse flows. However, the sinking of water masses, in balance with the upwellings, occurs in only a few locations around the world, including the North Atlantic and the Southern Ocean, around Antarctica (Whitworth et al., 1999). A

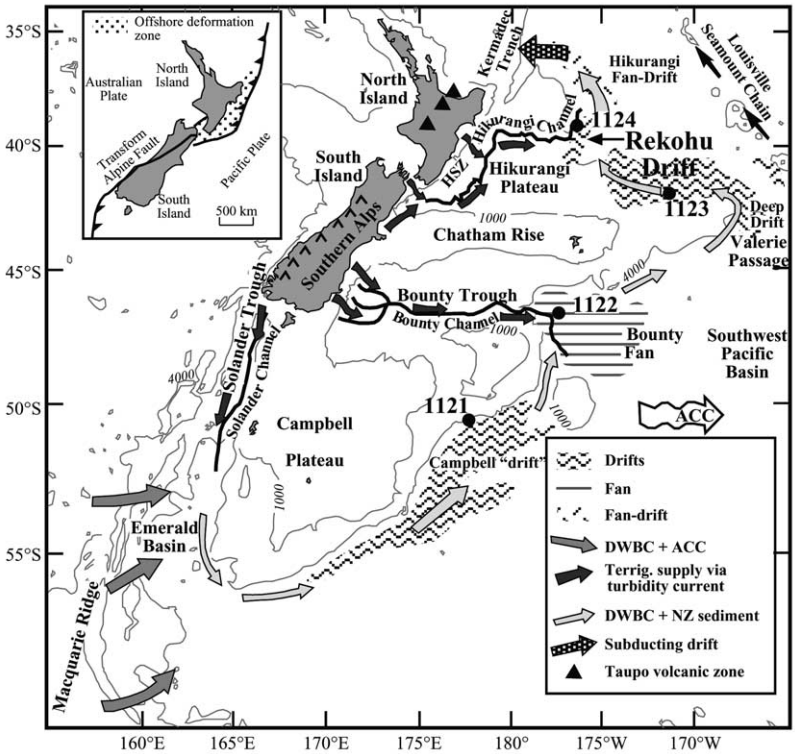

Fig. 1. Present sediment transport systems around the New Zealand area (from Carter et al., 1999). Contours in meters.

conservative estimate of production of Antarctic Bottom Water (AABW) is 8×10^6 m^3/s, but values range up to 13×10^6 m^3/s (Orsi et al., 1995, 1999).

The Southwest Pacific is a gateway through which approximately 40% of the deep waters enter the world's oceans from Antarctica, making its DWBC the largest single source of deep ocean water (i.e. Carter et al., 1996; Carter and Wilkin, 1999; Orsi et al., 1999). Presently, the ACC, and thus the DWBC as the deepest portion of the ACC, travels through the passage between Antarctica and Australia, within the Balleny Fracture Zone in the southeast Indian Ridge, before turning northeast at Macquarie Ridge (~60°S) into the Pacific Basin (Fig. 1; Carter et al., 1996; Carter and McCave, 1997; Orsi et al., 1999). At the mouth of the Bounty Trough (~50°S), the ACC and the DWBC uncouple, the ACC continuing in its eastward circuit and the DWBC traveling north. Bounded by the topography surrounding New Zealand, the 1000-km-wide DWBC flows along the 3500-m contour on the Campbell Plateau, around Hikurangi Plateau, to follow the Kermadec Trench northward (Carter and McCave, 1994; Carter et al., 1996, 1999). Estimates of strong and variable flow from current meters indicate transport of the DWBC east of New Zealand and the Kermadec Ridge to be approximately 16×10^6 m^3/s ($\pm11.9\times10^6$ m^3/s), with Circumpolar Deep Water (CDW) comprising 15.8×10^6 m^3/s ($\pm5.1\times10^6$ m^3/s). Pacific Deep Water (PDW) comprises the remainder (Warren, 1973; Whitworth et al., 1999).

2.2. The New Zealand microcontinent, continental margin, and tectonic development

The New Zealand microcontinent began moving away from Antarctica between ~80 and 60 Ma, incurring the formation of the Tasman Sea and part of the Pacific Ocean (Fig. 2; Kamp, 1986; Carter and Carter, 1987; Carter and McCave, 1997). During the early Oligocene, New Zealand was almost completely submerged and terrigenous sediment sources were buried or flooded (Rait et al., 1991; Carter et al., 1996, 1999).

The North and South Islands of New Zealand

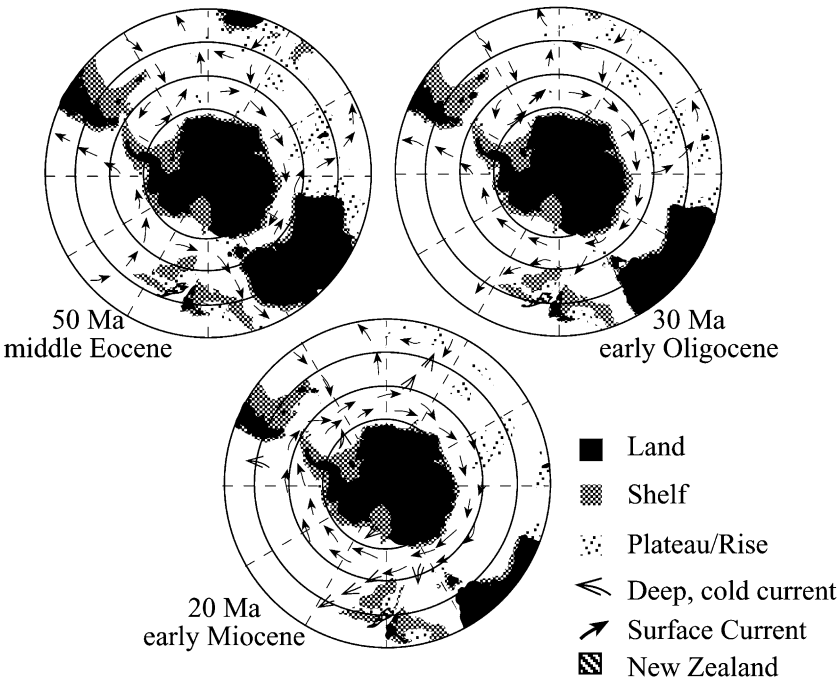

Fig. 2. Paleocirculation around Antarctica at 50, 30, and 20 Ma (from Carter et al., 1999; Lawver et al., 1992).

are cut by the Australian–Pacific plate boundary, accounting for the differences in ongoing geologic processes and topographies between the islands (Walcott, 1978; Carter et al., 1999). The Alpine Fault did not form on the western South Island until late Eocene; by early Miocene (~24 Ma) large amounts of sediment were shed from the rising mountains along the Alpine Fault. During the late Miocene (~6.5 Ma) there was an enhanced episode of uplift along the Alpine Fault (Carter and Norris, 1976; Carter et al., 1999 and refs therein). Currently, the Southern Alps are recognized as one of the fastest rising mountain belts in the world. New Zealand is thus a prominent sediment source to the oceans, providing 9% of the annual suspended fluvial input to the Southwest Pacific, ~2% to the oceans overall (Carter and McCave, 1997 and references therein). East of the North Island, the Hikurangi Subduction Complex (HSC; or Trough) is located where the Pacific plate is subducting under the North Island, resulting in the Central Volcanic Zone (Carter and Norris, 1976; Walcott, 1978; Carter et al., 1999).

2.3. Evolution of the ACC/DWBC systems

The opening of gateways to circumpolar oceanic circulation and deep water formation are influenced by plate tectonics and the associated movement of the continents away from Antarctica (Fig. 2). By ~43 Ma, the Australian block had moved far enough away from Antarctica to allow minor deep circulation through the Tasman Sea, although Tasmania and the South Tasman Rise still blocked deep water circulation. Around 34–30 Ma, the deep water connection between the Indian and Pacific oceans opened for the first time (Kennett et al., 1972; Kennett, 1977, 1980; Carter et al., 1996; Exon et al., 2001). While the Antarctic Peninsula moved eastward with respect to South America, the Drake Passage remained closed until about early Oligocene time (Kennett, 1977; Kennett and Stott, 1990; Lawver et al., 1992; Lazarus and Caulet, 1993; Veevers, 2000). Unrestricted latitudinal flow of the ACC, similar to today, was fully established by the early Neogene. The delay between the opening of the Drake Passage and the establishment of modern oceanic circulation may be due to the time required for deepening of the ocean basin between the continents, associated plateaus (e.g. Kerguelen), and Antarctica. Estimates of more specific time periods vary widely (Kennett, 1977; Kemp, 1978; Zachos et al., 2001).

Despite New Zealand's continuous tectonism, the offshore region of the eastern New Zealand plateau has been relatively unaffected by any major tectonic event since rifting in the late Cretaceous and has acted primarily as a trailing-edge passive margin (Carter et al., 1999). Flowing at bathyal to abyssal depths along the margin of New Zealand, the Southwest Pacific DWBC has influenced sediment erosion and deposition east of the New Zealand microcontinent (Fig. 1, Carter et al., 1996). Today this is evidenced by the presence of scoured bedrock, manganese nodule fields, and sediment drifts around the eastern continental boundary of New Zealand. The first evidence of widespread current activity and for significant sediment drift formation around the New Zealand margin occurred in the late Eocene/early Oligocene. The Marshall Paraconformity (~33–27 Ma), a regional unconformity noted by previous drilling legs as well as onshore studies, indicates that circulation was well established and vigorous by mid–late Oligocene (e.g. Carter and Landis, 1972; Kennett et al., 1972; Carter et al., 1996; Fulthorpe et al., 1996). The Southern Alps of New Zealand started to rise and shed sediment eastward through the Bounty Trough to the South Island continental margin during the Miocene, while below 2000 m water depth sediment drifts began to form (Carter et al., 1996).

One of the goals of this study is to use the properties of the sediment recovered from sediment drifts to investigate the establishment and fluctuations in the ACC and DWBC as they developed through ensuing major tectonic and climatic changes and reached modern intensities (Fig. 1; Carter et al., 1996, 1999). Potential sediment sources include New Zealand, Antarctica, and reworked southerly sediment drifts (Carter and McCave, 1994; Carter et al., 1996, 1999). This study focuses on the last 27 my of sediment collected at ODP Site 1124, the Rekohu sediment

drift near the mouth of the Hikurangi Channel (Fig. 1).

3. Study location

3.1. Rekohu Drift

The Rekohu Drift, a 250-km-long ridge-like feature of mainly Miocene and older sediment, is located approximately 600 km east of the North Island (Carter et al., 1996). The drift is built upon a volcanic basement ridge and currently acts to divert the DWBC and serves as an effective barrier/levee to the Hikurangi Channel (Fig. 1, Carter and McCave, 1994). Rekohu Drift lies between the Bounty Trough to the south and Kermadec Trench to the north and thus within the 'integrated sediment source-transport-sink area' of the eastern New Zealand Oceanic Sedimentary System (ENZOSS, e.g. Carter et al., 1996).

The Southwest Pacific DWBC that bathes Rekohu Drift, already decoupled from the ACC, has made its way north along the New Zealand continental margin passing two major sites of sediment injection, the Solander and Bounty Troughs (Carter and Mitchell, 1987; Carter et al., 1996). North of Chatham Rise, the DWBC is less energetic until it reaches the Rapuhia Scarp, but carries a larger sediment load. In addition to any terrigenous sediment that may have been carried this far north from the Antarctic Basin, these two sites are likely sources for Rekohu Drift sediment. Eroded drifts south of Rekohu Drift can act as significant sediment sources as well; upper Neogene sediment of Site 1124 contains reworked Eocene taxa likely released from the erosion of drifts lying further south (Schuur et al., 1998; Carter et al., 1999).

Large amounts of sediment are delivered from Kaikoura and Cook Strait canyons (less than 10 km from the coastal mountains and only a few hundred meters from the shore) to the continental margin via turbidity flows that move along the 1400-km-long Hikurangi Channel (Carter et al., 1996, 1999). This constant supply is brought to the mouth of the Hikurangi Channel, where the relatively accelerated DWBC sweeps sediment input into a 'fan-drift' – a fan deposit that has been extended 300 km downcurrent within the DWBC (Carter and McCave, 1997). In all 1200 m from the source, Hikurangi Channel is redirected northeast by the Rekohu Drift. Therefore, the Rekohu Drift may have as its sediment source turbidity currents overflowing the effective levee of Hikurangi Channel. Rekohu Drift formation predates the development of the Hikurangi Channel System which did not develop until Pliocene or even Pleistocene times when a submarine slide blocked the path of sediment directly to the Kermadec Trench (Carter and McCave, 1994; Lewis et al., 1998).

3.2. Site selection ODP Site 1124

ODP Site 1124 (39°29.901′S, 176°31.894′W, 3967 m below sea level) cored into the Rekohu Drift. Through the Oligocene, the core is comprised primarily of clay-bearing nannofossil oozes with tephra layers, which are more frequent and thicker (up to 90 cm) near the top of the core. The oldest noted tephra is located at approximately 207 m below sea floor (mbsf) and is of mid–late Miocene age (Carter et al., 1999, 2003). Samples extend through the Oligocene, however a number of hiatuses are present at approximately 28.4, 28.0, 27.1, 22.5–17.5, 16.5–15, and 14–11.1 Ma (Table 1). There are a few other small hiatuses as well as the 58–37 Ma hiatus that covers much of the Eocene and extends beyond our sampling zone (Carter et al., 1999).

Table 1
Ages of hiatuses from ODP Leg 181, Site 1124 (based on Carter et al., 1999)

Depth (mcd)	Start age (Ma)	End age (Ma)
440.93	58	37
>431.18	<37.0	33.6
>425.38	33.6	33.1
>422.80	<28.4	>28.0
>421.13	<28.0	>27.1
288.23	22.5	17.5
267.00	16.5	15.0
~237.50	14.0	11.1

Table 2
ODP Leg 181, Site 1124 age datums used for linear extrapolation of sample ages

Depth (mcd)	Age (Ma)
21.06	0.42
25.18	0.65
39.85	0.99
43.25	1.07
50.30	1.20
52.70	1.21
64.50	1.77
67.65	1.95
71.25	2.14
71.60	2.15
81.60	2.58
89.15	3.04
90.60	3.11
91.55	3.22
93.20	3.33
97.30	3.58
106.60	4.18
108.95	4.29
111.60	4.48
113.65	4.62
115.65	4.80
116.90	4.89
118.30	4.98
123.15	5.23
135.10	5.89
139.95	6.13
143.10	6.24
148.45	6.57
154.70	6.93
156.30	7.09
157.25	7.14
158.25	7.17
161.55	7.34
162.10	7.38
162.60	7.43
164.30	7.56
166.80	7.65
171.63	8.07
175.73	8.23
176.03	8.26
180.53	8.70
185.63	9.03
189.13	9.23
189.58	9.31
199.23	9.74
234.93	10.95
235.38	11.05
236.98	11.10
237.00	11.10
238.00	14.00
238.23	14.18
252.78	14.80
255.58	14.89
267.00	15.00
267.00	16.50
269.43	16.73
288.23	17.50
288.23	22.50
334.43	23.68
338.08	23.80
350.18	23.99
355.73	24.12
381.83	24.73
382.58	24.78
385.08	24.84
388.73	25.18
394.43	25.50
398.58	25.65
401.93	25.82
413.08	26.55
420.73	27.03
422.88	27.97
425.38	33.06
431.18	33.55
440.93	37.00
440.93	58.00
458.71	62.50
472.68	64.75

The youngest two datums were determined through biostratigraphy while the remaining datums are magnetostratigraphic. Depths are provided in meters composite depth (mcd; Carter et al., 1999).

4. Methods

In all 272 separate samples of the Rekohu sediment drift (adjacent scoop samples and $2.2 \times 2.1 \times 1.4$ cm paleomagnetic cubes) were obtained from ODP Site 1124B, C, and D cores. Care was taken to avoid sampling discrete ash layers, however, dispersed ash was pervasive in the top portion of the core.

4.1. Terrigenous sediment characterization

4.1.1. Chemical extraction

Scoop samples were subject to a chemical extraction process based on the procedures described by Rea and Janecek (1981) with modifications by Clemens and Prell (1990) and Hovan

(1995). This process removes calcium carbonate, oxides and hydroxides, zeolites, and biogenic silica in order to isolate the terrigenous mineral component of marine sediment; however, it should be noted that ash survives this procedure. The terrigenous wt% is calculated by comparing the weight of each sample before and after chemical extraction. The age model is based on linear extrapolation primarily using both paleomagnetic and biostratigraphic data from the ODP Leg 181 Initial Results Volume (Table 2; Carter et al., 1999, 2003).

4.1.2. Terrigenous mass accumulation rates

Terrigenous mass accumulation rates (MAR) in g/cm^2/ky were calculated using the equation:

$$\text{Terrigenous MAR} = \text{LSR} \times \text{DBD} \times \text{terrigenous weight \%}$$

where LSR is the linear sedimentation rate (in cm/ky), DBD is the dry bulk density (in g/cm^3) obtained from shipboard bulk density values, and the terrigenous wt% is determined using the chemical extraction method provided above. As a result, the history of terrigenous input is independent of dilution/concentration effects incurred by variations in input rates of other sediment components, a difficulty often encountered when using only percentage data.

4.1.3. Terrigenous grain size

Grain size analysis was performed on the extracted terrigenous component using a Multisizer IIE Coulter Counter with a selected analysis range between 2 and 100 μm. Terrigenous median grain size is represented here using both microns and Φ units (Φ_{50}; $\Phi = -\log_2(\text{grain diameter}_{mm})$).

4.2. Magnetic fabric analysis

Anisotropy of magnetic susceptibility (AMS) analyses were conducted on paleomagnetic cube samples using a KLY-2 KappaBridge. Results of AMS analyses show the bulk orientation of all grains in a sample, called the magnetic fabric, and are represented in 3-D space by an ellipsoid; in most cases the greatest induced magnetization parallels the long axis (Nye, 1957; 1985; Tarling and Hrouda, 1993 and references therein). The parameter P' mathematically represents the degree of anisotropy of the resulting magnetization ellipsoid (greater P' values represent a more developed anisotropy of the magnetization ellipsoid) and the parameter T represents the shape factor of the ellipsoid. When $0 < T \leq 1$, then the ellipsoid is oblate while if $-1 \leq T < 0$, the ellipsoid is prolate.

Previous studies (e.g. Rea and Hovan, 1995; Boven and Rea, 1998; Joseph et al., 1998) have provided robust methods by which the mode of terrigenous sediment transport and deposition can be determined by appropriate analyses of a single sample using a combination of AMS and terrigenous grain size analyses. Grains deposited by moving water, such as with sediment drifts and turbidites, show a distinct magnetic fabric; those deposited by random settling, eolian, pelagic, or hemipelagic, show no grain alignment along the long axis. The terrigenous grain size distributions allow discrimination between drift vs. turbidite, and eolian vs. hemipelagic deposition. In general, coarser median grain sizes combined with higher P' values indicate stronger depositional energies, however, due to source effects, it is sometimes necessary to rely more heavily on one parameter.

5. Results

Terrigenous MARs vary between near zero to almost 10 g/cm^2/ky, but are most commonly between ~0.5–2.5 g/cm^2/ky (Figs. 3 and 4). Terrigenous median grain size varies between ~7.5 and 6.0Φ and appears to increase in variability upcore while maintaining a base value of approximately 7.5Φ throughout the interval sampled.

The middle–late Oligocene (~27 Ma) through early Miocene period (~23 Ma) exhibits an increase in terrigenous MARs from <0.5 to ~3 g/cm^2/ky, in a trend somewhat similar to that of the bulk magnetic susceptibility and terrigenous wt% (Figs. 4 and 5). Median terrigenous grain sizes exhibit two peaks in coarseness at ~26.3 and 23.8 Ma. Over this interval, carbonate wt% declines from nearly 80% at 27 Ma to less than

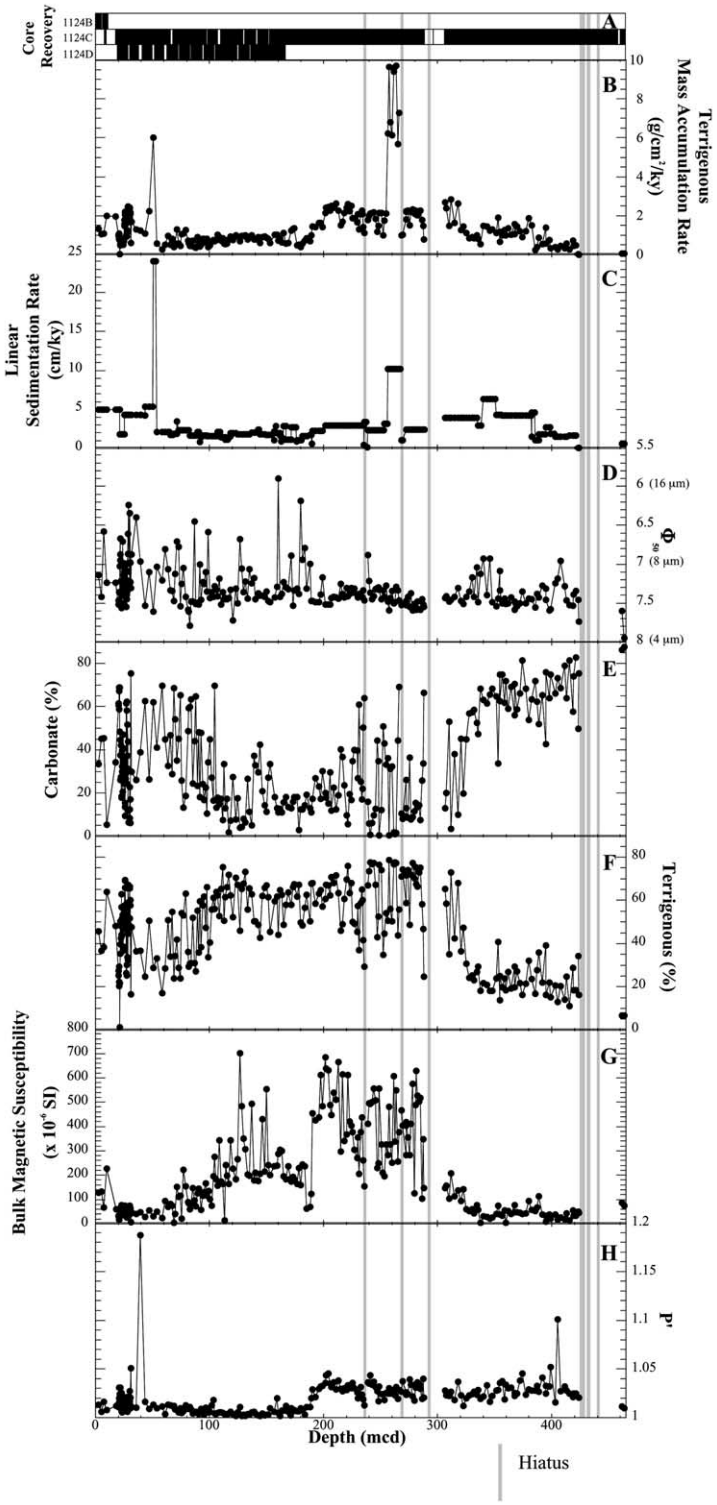
Core Recovery
1124B
1124C
1124D
A
B
Terrigenous Mass Accumulation Rate (g/cm²/ky)
C
Linear Sedimentation Rate (cm/ky)
D
Φ 8s
6 (16 μm)
7 (8 μm)
8 (4 μm)
E
Carbonate (%)
F
Terrigenous (%)
G
Bulk Magnetic Susceptibility (x 10⁻⁶ SI)
H
P'
Depth (mcd)
Hiatus

30% at 23 Ma, changing most significantly between 24 and 23 Ma.

Most of the early–middle Miocene was characterized by periods of non-deposition or erosion (chemical or physical), represented in the form of hiatuses (Fig. 4). The interpretation of the 22.5–17.6-Ma hiatus is complicated by the lack of recovery; however, if deposition was continuous during this time period, LSRs would be comparatively very low at ~0.4 cm/ky.

Two small glimpses into the middle Miocene sediment drift environment are present between the hiatuses. In both intervals, the MARs remain generally high, resulting from high calculated LSRs and large terrigenous wt%. Bulk susceptibilities have increased and range up to 600×10^{-6} SI and magnetic fabrics (P') remain strong. Carbonate content is generally low, with more variation in the younger interval. Median grain size is relatively fine, averaging around 7.6Φ in the older interval and coarsening slightly upcore through the younger interval. The extremely high MAR values at 15 Ma (as well as 1.2 Ma) result from a short interval of very high calculated LSR, and likely are an artifact of the resolution of the timescale datums (Fig. 4A,B).

The late Miocene (~11–5.5 Ma) has an initial 2-my period where MARs, bulk magnetic susceptibility values and P' values exhibit a distinct rise to a maximum at 10 Ma, followed by a drop in values comparable to, or lower than, those in the middle Oligocene (Figs. 4 and 6). This pattern is mimicked by the terrigenous wt%, although in a muted form. Carbonate wt% values are initially larger than those in the mid-Miocene and show a decline in values from 11 to 9 Ma. Terrigenous grain size clusters tightly at ~7.5Φ until 10 Ma, then coarsen slightly, with much more variation, until around 7 Ma.

MARs, carbonate wt%, and P' values remain very low and fairly constant for the remainder of the Miocene, while terrigenous wt% values remain high. However, the bulk magnetic susceptibility shows a gradual increase upcore to a relative high around the time of the Miocene–Pliocene boundary (~5 Ma). The first tephra layer occurs at around 11.16 Ma (207 mbsf; Carter et al., 1999, 2003).

MARs of the terrigenous component remain very low (<1 g/cm^2/ky), as do P' values, during the Pliocene interval (~5.5–1.8 Ma). Bulk susceptibilities and terrigenous wt% values gradually decrease, while the carbonate wt% values gradually increase during this interval. The median grain size is finer between ~5 and 4 Ma, followed by a general increase in both grain size and grain size variability through the end of the Pliocene.

During the Pleistocene, MARs vary up to 2 g/cm^2/ky and P' values initially rise slightly. Bulk magnetic susceptibilities remain under 100×10^{-6} SI, except at the coretop. The carbonate weight abundance decreases in the past 1 my, while individual measurements exhibit a great deal of variability between 5 and 80%. Grain size is also quite variable during the Pleistocene, varying between 7.6 and 6.3Φ.

Sediment deposited around the time of the Bruhnes–Matuyama boundary (0.78 Ma; Cande and Kent, 1995) was sampled more intensively to provide a high resolution sequence with which to investigate the presence (or lack) of an orbitally-forced sediment signal. Fig. 7 shows the sediment parameters plotted on an orbitally-tuned timescale determined for Site 1123, tied to the Site 1124 record using proxy carbonate data (Hall et al., 2002). Between 0.8 and 0.5 Ma, MARs, initially at ~2 g/cm^2/ky, drop to <1 g/cm^2/ky at ~0.64 Ma and remain there for the rest of the interval. Carbonate wt% values show a several-fold fluctuation, and overall show a generally increasing trend from 0.74 to 0.5 Ma, mirrored by the terrigenous wt%. Terrigenous median grain sizes are very variable throughout, while bulk magnetic susceptibility shows almost no variation from its low values $<100\times10^{-6}$ SI. P' values are also fairly low and constant throughout

Fig. 3. Results of sediment characterization from Site 1124. Core recovery (A) represented in black, non-recovery in white (Carter et al., 1999), trends in terrigenous MAR (B), linear sedimentation rate (C), terrigenous median grain size (D), carbonate wt% (E), terrigenous wt% (F), bulk magnetic susceptibility (G), and magnetic fabric (H) at Site 1124 for ~460 mcd.

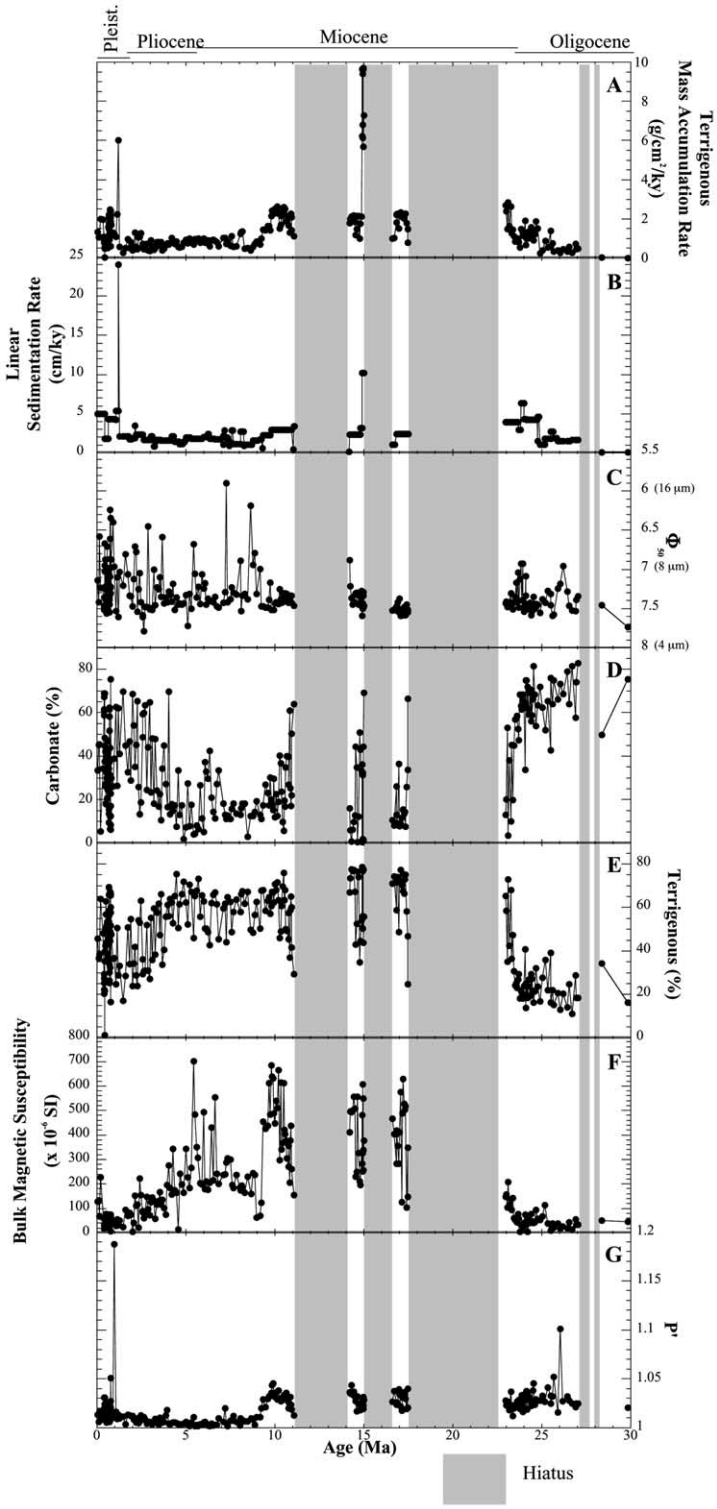
Pleist.
Pliocene
Miocene
Oligocene
A
Terrigenous Mass Accumulation Rate (g/cm²/ky)
B
Linear Sedimentation Rate (cm/ky)
C
Φ
(16 µm)
(8 µm)
(4 µm)
D
Carbonate (%)
E
Terrigenous (%)
F
Bulk Magnetic Susceptibility (x 10⁻⁶ SI)
G
P'
Age (Ma)
Hiatus

the interval, showing an increase at approximately 0.58 Ma.

6. Discussion

Overall, five distinct intervals are noted based on the sediment parameters described above. The breaks between these intervals are at 24.5, 9.0, 5.8, and 1.5 Ma. Depositional environmental determinations using magnetic fabric and terrigenous grain size parameters were constructed for each of these units separately and are provided in Fig. 8A–E. Overall, the terrigenous median grain size, which is generally fine throughout, plots primarily in the low-energy environment field, while the magnetic fabrics vary between those characteristic of low- and middle-energy (pelagic interlayer and sediment drift types, respectively) depositional environments. In general, P' values increase from relative lows after hiatuses and exhibit an increase just prior to hiatuses. Terrigenous median grain size exhibits a distinct baseline at $\sim 7.5\Phi$ throughout the entire record (Figs. 3 and 4). This likely represents either a source effect or an effect of the travel path and distance, rather than localized sluggish current transport as the magnetic fabric indicates significant current influence in the older portion of the record.

6.1. 27–24.5 Ma: strong and fluctuating DWBC

The interval between 27 and 24.5 Ma is characterized by low bulk magnetic susceptibilities, terrigenous wt% values, and MARs (Figs. 4 and 5). However, terrigenous grain sizes are variable and P' values are relatively high. The magnetic fabrics suggest a pronounced sediment drift-like environmental energy while terrigenous deposition remains relatively low.

This interval in the late Oligocene before any major New Zealand tectonic uplift, following two mid-Oligocene hiatuses, likely represents the slowing down of the DWBC to non-scouring, depositional velocities. The flow, however, remains strong, as indicated by the magnetic fabric, although median grain sizes are fine.

6.2. 24.5–9.0 Ma: continued strength of the DWBC

The latest Oligocene through the late Miocene is a period of strong and variable current activity. This is evidenced not only by the three major episodes of non-deposition/scouring of sediment, but also by strong magnetic fabrics and large terrigenous inputs between hiatuses (Fig. 4).

In the latest Oligocene–earliest Miocene, terrigenous input increases gradually while P' values decrease slightly, although fabrics still remain strongly oriented. This is indicative of either a continued slowdown of the Pacific DWBC possibly with an increased supply of material, allowing for drift deposition while still maintaining strong flows.

The presence of hiatuses through increased corrosiveness or physical erosion (or non-deposition of sediment) is largely influenced by the path of bottom water flows and changes in the intensity of ocean circulation (Keller and Barron, 1983). The hiatuses noted in this study, with the windows of time recorded between them, imply a strong, but variable DWBC throughout the early–middle Miocene, with episodes of erosion/non-deposition followed by periods when either the DWBC decelerated, indicated by the relatively weak magnetic fabric values immediately after hiatuses, and/or sediment supply increased enough to allow significant deposition.

Between the youngest hiatus and 9 Ma, a peak in MARs, P', and bulk magnetic susceptibility at 10 Ma is quite distinctive (Figs. 4 and 6). In this interval, the magnetic fabrics become more oriented in concert with the higher terrigenous input, implying a greater amount of deposition within a faster current. Here, following a slowdown of the

Fig. 4. Results of sediment characterization from Site 1124. Trends in terrigenous MAR (A), linear sedimentation rate (B), terrigenous median grain size (C), carbonate wt% (D), terrigenous wt% (E), bulk magnetic susceptibility (F), and magnetic fabric (G) at Site 1124 for ~ 30 My.

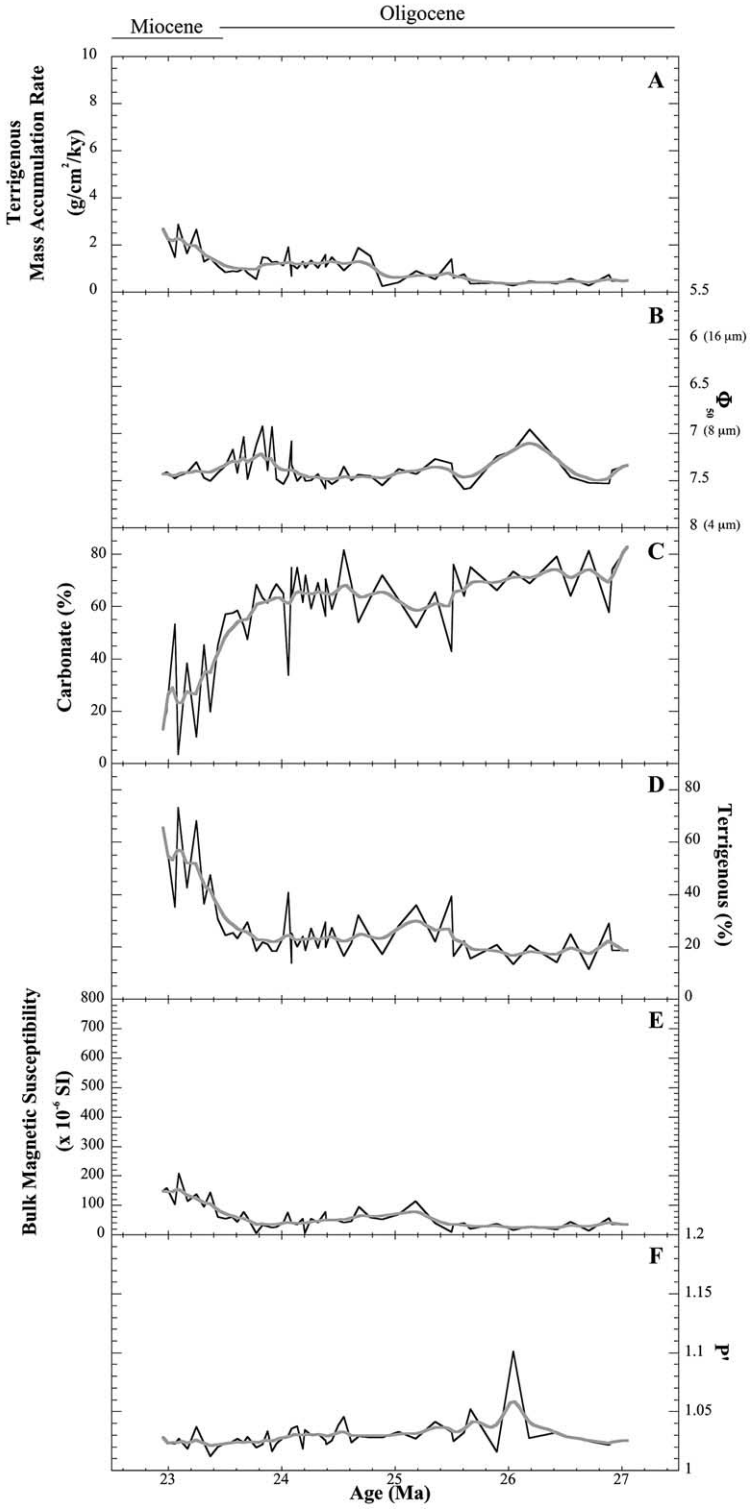
Miocene
Oligocene
Terrigenous Mass Accumulation Rate (g/cm²/ky)
A
B
Φ
6 (16 μm)
6.5
7 (8 μm)
7.5
8 (4 μm)
Carbonate (%)
C
D
Terrigenous (%)
Bulk Magnetic Susceptibility (x 10⁻⁶ SI)
E
F
P'
Age (Ma)

DWBC from scouring intensities that created the hiatus, the comparison of maxima in sediment properties indicates that the current has become stronger once again around 10 Ma (Fig. 6). A major increase in sediment transport to the DWBC upcurrent of Rekohu Drift may surpass the carrying capacity of the water mass and deposition may result at continued high velocities. This terrigenous input peak may represent more extensive erosion of sediment upcurrent from Rekohu Drift. It is also possible that the increase in terrigenous input at about 10 Ma reflects increased injection of sediment from the mountains of New Zealand to the deep-sea channel/fan systems (Carter et al., 1996), possibly through the Solander or Bounty channels. However, an hiatus was noted at Site 1122 (Bounty Fan) from ~10 to 4 Ma and turbidite deposition did not occur at the Bounty Fan until approximately the early Pleistocene, implying that at least this path had not yet reached the influence of the DWBC (Carter et al., 1999).

6.3. 9.0–5.8 Ma: lack of current influence and low terrigenous input

After 9 Ma a decline in sediment dry bulk density occurs: this is the boundary between lithologic units 1C and 1B where nannofossil ooze and silty clay change downsection to nannofossil chalk and mudstone (Carter et al., 1999). Determinations of MARs, however, take this factor into consideration. Although the terrigenous wt% is high (showing an inverse variation with carbonate wt%), the terrigenous MARs remain low and steady between 9 and 5.8 Ma, despite the potential enhancement in the MARs from ash input and other increases in sediment supply likely to have been associated with intensified collision along the New Zealand plate boundary (Carter et al., 1999 and references therein; Carter et al., 2003). This implies that the additional sediment generated by these processes did not have a pathway to Rekohu Drift; the Hikurangi Channel was not yet directed eastward and the Bounty Fan Channel did not yet reach the DWBC's influence. Terrigenous grain sizes remain fine and the increased variability in median grain sizes may result from the introduction of ash as part of the terrigenous component. McCave and Carter (1997) noted a relatively coarse grain size in the modern sediment of Rekohu Drift that likely resulted, at least partially, from the presence of the Taupo ash.

Some complications exist for the remaining portion of the record. An initial macroscopic tephra layer occurs around the start of the late Miocene, representing the onset of volcanism on the North Island of New Zealand. Once volcanism begins, the ash input to the sediment record becomes significant with ash layers (>1 cm) making up 6% of the late Miocene and younger sediment column. These ash layers provide a wonderful opportunity for dating as well as correlation of New Zealand shore-based studies of volcanism (Carter et al., 1999, 2003). However, because ash cannot be removed by the extraction process used in this study, it causes complications in determining both depositional environment and terrigenous input. Peaks in bulk magnetic susceptibilities do not appear to correspond with visible ash layers. Although care was taken not to sample tephra layers, glass was still visible in smear-slides of many post-extraction samples and is likely present in the sediment column as dispersed ash or microscopic tephra layers.

P' values, the magnetic fabric, are very low values between 9 and 5.8 Ma, indicating the lack of current influence (or a very small one) at this time. It is possible that this drop in P' values at 9 Ma represents only the lithologic change from more to less consolidated sediment; however, this is a significant drop to consistently low values. Previous studies using unconsolidated sediment

Fig. 5. Expanded version of the period between 27.5 and 22.5 Ma. Terrigenous MAR (A), terrigenous median grain size (B), carbonate wt% (C), terrigenous wt% (D), bulk magnetic susceptibility (E), and magnetic fabric (F). The black line represents the distinct data points, the gray line is smoothed. The smoothed curves have the geometric weight applied to the current point and ±10% of the data range.

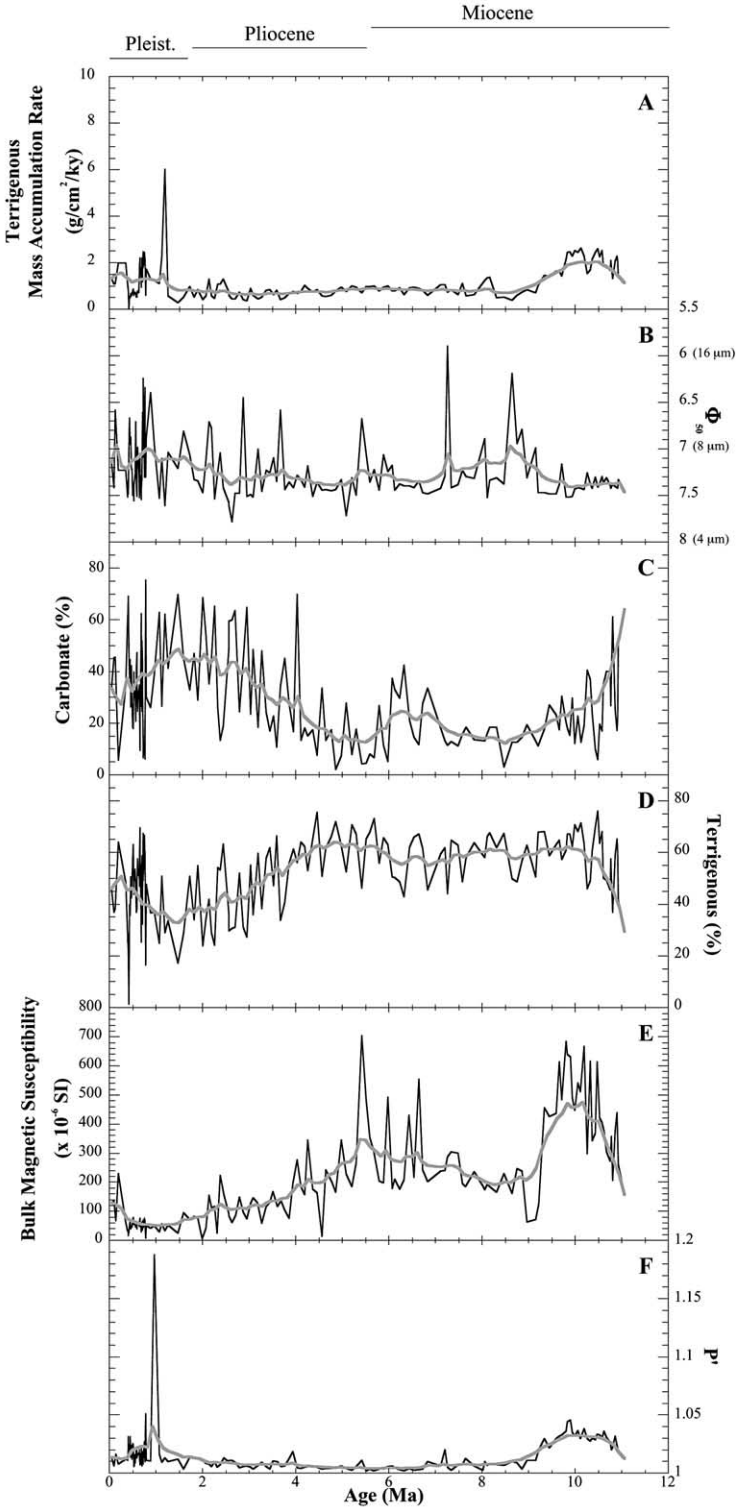
Pleist.
Pliocene
Miocene
Terrigenous Mass Accumulation Rate (g/cm²/ky)
A
B
Φ
6 (16 μm)
7 (8 μm)
8 (4 μm)
C
Carbonate (%)
D
Terrigenous (%)
E
Bulk Magnetic Susceptibility (x 10⁻⁶ SI)
F
P'
Age (Ma)

from drifts and turbidites (Joseph et al., 1998) show higher P' values in similar sediment, indicating the presence of currents.

While bulk magnetic susceptibility and extracted terrigenous wt% trends mimic each other, the terrigenous wt% trend is muted in comparison to the bulk magnetic susceptibility. This may also be a result of the addition of the ash component to the system and the various effects the introduction of ash would impose on each of these analyses.

6.4. 5.8–1.5 Ma: ash and the Hikurangi Channel influence

Ash is a significant component of the Pliocene section at Site 1124 as well. In all 41 visible tephra layers were noted with this age interval, averaging approximately one layer every 1.4 m (Carter et al., 1999, 2003).

The formation of the Hikurangi Channel may have occurred during the Pliocene or early Pleistocene (Lewis et al., 1998; Carter et al., 1999). The formation of this channel altered the sediment distribution pathways of the Kaikoura Canyon (located at the foot of the coastal mountains) and Northern Island areas from the Hikurangi Trough (or subduction complex), cutting across the Hikurangi Plateau to the continental margin. Currently, Rekohu Drift acts as an effective barrier to the Hikurangi Channel turbidity flows and overbank flow from the channel onto the drift has likely occurred. Despite this potential additional input to the terrigenous MAR of this sediment drift, the terrigenous fluxes remain low through the late Pliocene, and the magnetic fabric is consistently weak. As carbonate wt% increases, terrigenous wt% and bulk magnetic susceptibility show the corresponding decline expected in a two-component system. The increasing variation in terrigenous grain size likely represents the combination of ash and hemipelagic muds. This time period is typified by low terrigenous input to the site, implying that interpretations of a later (early Pleistocene) formation of the channel (Lewis et al., 1998) is favored. Bottom flow energy, as measured by the magnetic fabric, is quite low.

6.5. < 1.5 Ma: tephra

The youngest 1.5 my of the record at Site 1124 exhibits some increased variation in sediment parameters. MARs increase slightly, as do terrigenous wt% values, yet bulk magnetic susceptibility values generally decrease (Fig. 4). Magnetic fabric data suggest that depositional energies vary between low and moderate velocities (Fig. 8).

Gradually increasing in depositional episodes, ash is even more of a complicating factor than during the proceeding time period (5.8–1.5 Ma), averaging one macroscopic tephra layer every 1.2 m and including some thicker layers (mean thickness 13.6 cm, maximum thickness 92 cm; Carter et al., 1999, 2003). The presence of ash in this section of the Pleistocene sediment may be responsible for the differences in the trends of bulk magnetic susceptibility and extracted terrigenous wt%, two independent measurements of terrigenous content. Significant ash contribution could also affect magnetic fabrics.

The interval around the Bruhnes–Matuyama boundary (0.3–0.8 Ma), a generally cold episode representing the initiation of high amplitude changes in ice volume with primarily 100-ky frequencies, experienced an enhanced ACC and bottom water flow according to previous studies (i.e. Bandy et al., 1971; Kuijpers, 1989). The time period was sampled at a higher resolution with the intention to investigate Milankovitch forcing of New Zealand climate. While this site is likely recording the climatic history of New Zealand, before this determination can be made the ash should be removed from the samples, new MAR's calculated, and terrigenous median grain sizes re-

Fig. 6. Expanded version of the period younger than 12 Ma. Terrigenous MAR (A), terrigenous median grain size (B), carbonate wt% (C), terrigenous wt% (D), bulk magnetic susceptibility (E), and magnetic fabric (F). The black line represents the distinct data points, the gray line is smoothed. The smoothed curves have the geometric weight applied to the current point and ±10% of the data range.

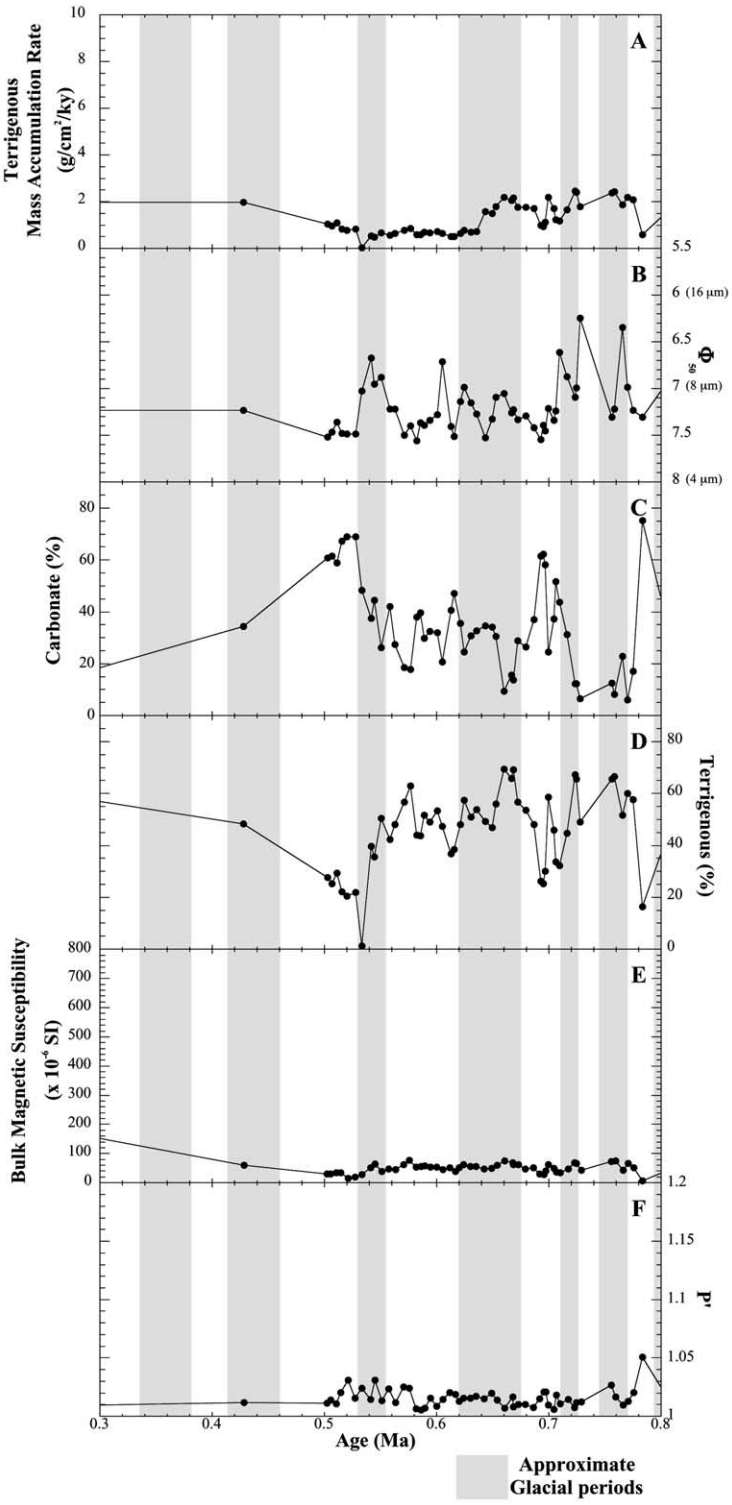
Terrigenous Mass Accumulation Rate (g/cm²/ky)
A
B
Φ50
6 (16 μm)
7 (8 μm)
8 (4 μm)
Carbonate (%)
C
D
Terrigenous (%)
Bulk Magnetic Susceptibility (x 10⁻⁶ SI)
E
F
P'
Age (Ma)
Approximate Glacial periods

analyzed. Hall et al.'s (2001, 2002) examination of southerly New Zealand ODP Sites 1123 and 1124 generally indicates coarser grains, increased carbonate dissolution, and a higher terrigenous input to these sites during glacial periods, although some major pulses noted at Site 1123 were missing or muted at Site 1124. Currently, some of our sediment parameters from Site 1124 show a possible correlation to glacial–interglacial cycles in Fig. 7 when plotted with $\delta^{18}O$ of benthic foraminifera from Site 1123 over 1.2 Ma (Hall et al., 2001), but as mentioned above, more detailed work needs to be completed.

6.6. Implications

Changes in the velocity of the Southwest Pacific DWBC will reflect changes in the intensity of bottom water production around Antarctica, particularly as the Southwest Pacific DWBC is the largest single source of bottom water to the world's oceans (i.e. Carter et al., 1996; Stickley et al., 2001). Bottom water production, in turn, is linked to circulation around Antarctica, climatic conditions, ice sheet coverage and stability and the presence of sea ice (i.e. Keller and Barron, 1983; Carter et al., 1996). Studies of various sediment parameters during more recent periods link glacial intervals around New Zealand to increased bottom water production from Antarctica (i.e. Hall et al., 2001, 2002; Stickley et al., 2001).

The record representing the period between 27 and 9 Ma shows the presence of a strong DWBC at the depth of Site 1124. Whereas the hiatuses make it difficult for exact interpretations, the MARs are generally consistently high, 1.5–2 g/cm^2/ky (between the hiatuses) starting at approximately 23 Ma. In a similar fashion, other sediment parameters are consistent throughout this interval. Thus, while the proto-ACC and deep waters have been forming since the early Oligocene, the full establishment of this system to modern circulation patterns likely occurred at ~23 Ma as deepening of the gateway between South America and the Antarctica Peninsula (the Drake Passage) continued. This generally corresponds with others estimates of ACC establishment, completing the thermal isolation of Antarctica and allowing for significant bottom water formation (Kennett, 1977; Lawver et al., 1992; Zachos et al., 2001).

Evidence exists from the Antarctic continent and offshore Antarctica of significant variation in ice-volume before and after the middle Miocene (e.g. Webb and Harwood, 1991 and references therein; Carter and McCave, 1994; Flower and Kennett, 1994, 1995; Zachos et al., 2001) and these fluctuations are reflected in the record of DWBC velocities provided by this study. Late Oligocene warming, as indicated by oxygen isotopes, begins ~28 Ma and reaches its initial maximum just after 27 Ma (Wright and Miller, 1993). This warming may have caused the DWBC to slow down enough to allow deposition. Climate begins to degrade ~25 Ma and the first major Miocene glacial period (Miocene isotope-1 [Mi-1]) occurs around 23 Ma, giving rise to the first erosional/non-depositional period of the Miocene. The peak in MAR's at 24 Ma, associated with slightly slower currents based on P' values is interpreted as the increase in terrigenous material coming from the rising mountains along the Alpine Fault boundary (Carter et al., 1999) although its exact pathway from New Zealand is uncertain.

The hiatus between ~22.5 and 17.5 Ma, resulting from erosion, carbonate dissolution or low sedimentation rates, is interpreted as a time of increased bottom water formation and thermohaline circulation. A widespread hiatus was noted by Keller and Barron between ~21 and 17 Ma, (NH1, accounting for timescale differences). While this is a relatively warm episode climati-

Fig. 7. Expanded version of the Bruhnes–Matuyama boundary plotted on an orbitally-tuned timescale determined for Site 1123, tied to the Site 1124 record using proxy carbonate data (Hall et al., 2002). Terrigenous MAR (A), terrigenous median grain size (B), carbonate wt% (C), terrigenous wt% (D), bulk magnetic susceptibility (E), and magnetic fabric (F). Sampled at higher resolution. Glacial periods determined from $\delta^{18}O$ values from Site 677, representing glacial periods 10–22.

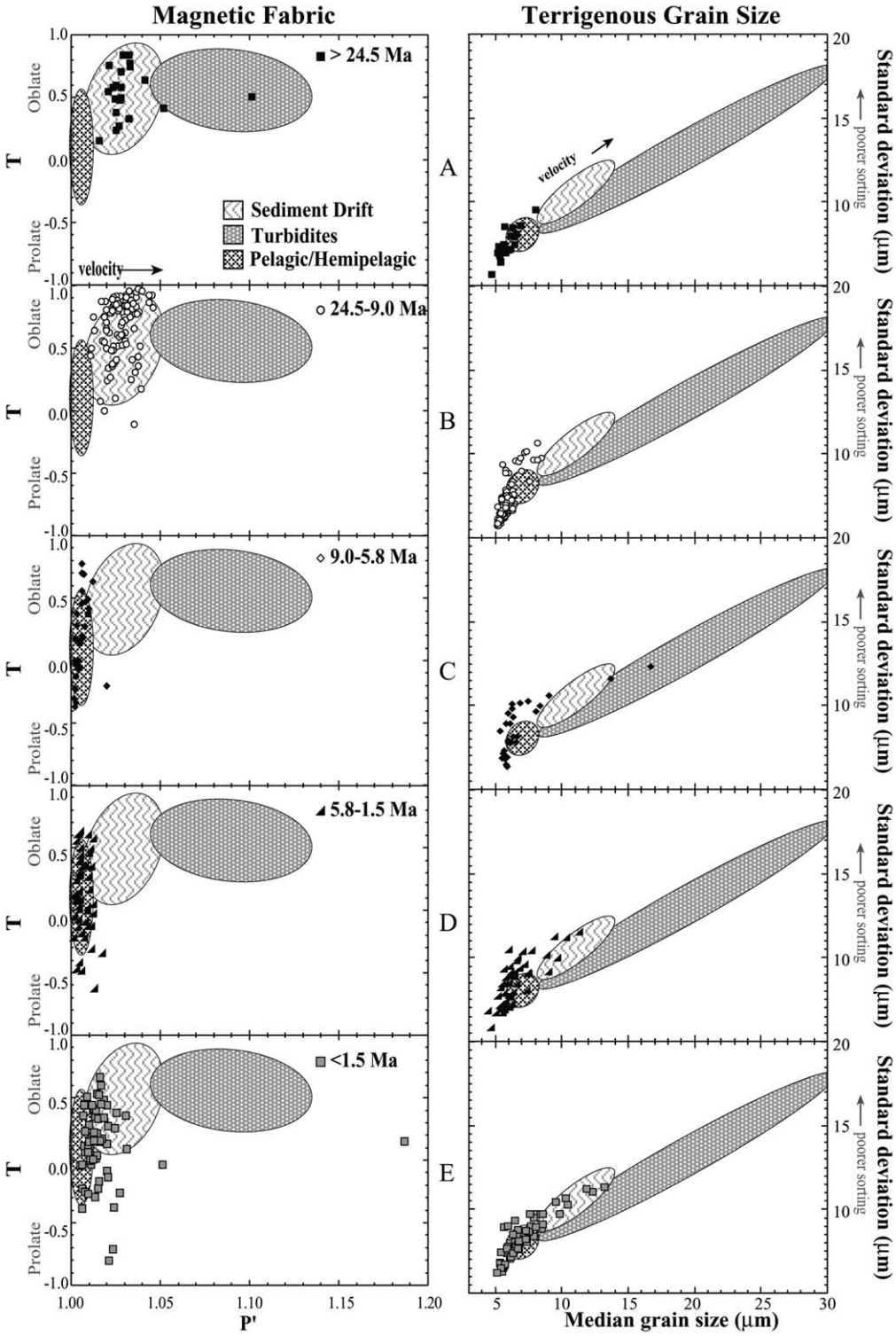
Magnetic Fabric
Terrigenous Grain Size
> 24.5 Ma
24.5-9.0 Ma
9.0-5.8 Ma
5.8-1.5 Ma
<1.5 Ma
Sediment Drift
Turbidites
Pelagic/Hemipelagic
velocity
Oblate
Prolate
T
P'
A
B
C
D
E
Standard deviation (μm)
poorer sorting
Median grain size (μm)

cally, Kennett (1995) suggests that this unusual connection between warm climates and increased intensity of Antarctic circulation results from the complete establishment of the ACC and the Polar Front Zone just prior to this time period. The effect of this is to isolate the Antarctic system from significant warming in the north.

The period from 17 to 14.5 Ma is generally warm, although oxygen isotope high Mi-2 occurs near the midpoint of this interval, an interval of increased deep water production occurred at ~15 Ma (Wright and Miller, 1993), and changing circulation patterns were noted by Keller and Barron (1983) between ~16.5 and 15 Ma (NH2). The glacial period probably stimulated the intensity of the DWBC and caused non-deposition or erosion between 16.5 and 15 Ma. The warmer periods are likely associated with records of high MARs and strong magnetic fabric, indicating a sediment supply that exceeded the carrying capacity of the current, yet the current was fast enough to leave its signature in the form of magnetic fabric. A recent study by Hall et al. (2003) on nearby Site 1123 indicates DWBC intensification during 15.5–12.5 Ma due to increased production of Southern Component Water.

The final Miocene hiatus between ~14 and 11 Ma at Site 1124 is associated with major expansion of the East Antarctic Ice Sheet; a shift in $\delta^{18}O$ of nearly 1.0‰ to more positive values occurs during this interval (Flower and Kennett, 1993; Wright and Miller, 1993; Kennett, 1995). A widespread hiatus (NH3) was noted at approximately 12.5–11.6 Ma (Keller and Barron, 1983). The expansion of the East Antarctic Ice Sheet would be expected to strengthen both atmospheric and thermohaline circulation, the latter through enhanced bottom water formation and ACC coupling with the DWBC.

At the beginning of the late Miocene, the period from 11 to 9 Ma exhibits some of the most positive $\delta^{18}O$ values of the entire Miocene and corresponds with a significant sea-level drop. The West Antarctic Ice Sheet was growing and establishing itself, although highly unstable during the late Miocene (e.g. Haq et al., 1987; Kennett, 1995). This growth would be expected to have had a significant impact on bottom water formation. The sediment record provided here indicates not only an increase in MARs at this time, but also an enhancement of the strength of magnetic fabric. At the peak of terrigenous input, the currents are the strongest, as opposed to the trend at 25–23 Ma when increases in measures of magnetic fabric are associated with decreases in terrigenous flux. The increase in terrigenous input at this site may have resulted from significant Antarctic erosion by the WAIS, which contributed significant sediment amounts to the Weddell and Bellinghausen abyssal plains and likely to the Ross Sea area as well (Kennett, 1995). Analysis of sediment from Kerguelen Plateau (Site 744) also indicates a significant increase in MARs at ~10 Ma (Joseph, 2001). However, although diatom tracers from Antarctica are present in New Zealand sediment drifts (Stickley et al., 2001), this path may be too long for large amounts of the denser terrigenous grains to travel. Another possible source includes the increase in sediment supply from New Zealand noted at ~10 Ma (e.g. Carter et al., 1996); provenance studies would help resolve the true source, or sources, of this increase in terrigenous flux. A warming following this cold episode lasted to ~7 Ma (Kennett, 1995).

The distinct lack of current influence at Site 1124 from 9 Ma to the present does not indicate that the DWBC is effectively non-existent, especially as its modern presence has been confirmed through physical oceanography (i.e. McCave and Carter, 1997). Site 1121, which is located directly

Fig. 8. Environmental velocity determinations using magnetic fabric (left) and grain size (right) parameters (see Joseph et al., 1998). (A–E) represent different time slices (oldest to youngest), determined from changes in the trends of the data in Fig. 4. The small shapes are the results from ODP Site 1124 samples, while the larger shaded areas behind them indicate previously defined energy fields (Joseph et al., 1998). The pelagic/hemipelagic field indicates a low energy depositional environment, the sediment drift field indicates a moderate energy, and the turbidite field indicates a high energy environment.

in the path of the ACC before it decouples from the DWBC, exhibits an hiatus over 50 my between ~56 to 1.5 Ma, representing significant current strengths at times within this period, and necessarily in the youngest portion. Sediment from Site 745 (Joseph et al., 2002), indicates variable and unstable ice sheets present on Antarctica until around 4 Ma, with the ice sheet becoming well established near sea level since then. Thus, one would expect fluctuations in the DWBC as ice sheet fluctuations near the coastline affect deep water formation. Other records indicate a flow-speed maximum in the same general area as Site 1124 at ~8.4 Ma, likely due to the formation of the West Antarctic Ice Sheet (Carter and McCave, 1994). Therefore, the lack of current influence at Site 1124 is a localized effect, possibly due to a small shift of the core of the current from the location of Site 1124. Thus the interval between 9 and 1.5 Ma at Site 1124 more likely represents variations in New Zealand history and evolution, rather than that of the DWBC. Fluctuations in sediment parameters may correspond to glacial/interglacial episodes however, reanalysis of the data after the removal of ash may aid these interpretations as would determination of terrigenous provenance.

7. Conclusions

Through the use of sediment characteristics, including terrigenous flux calculations, terrigenous grain size analysis, magnetic fabrics, and the timing of erosional/non-depositional events, the history of the Southwest Pacific DWBC between ~27 and 9 Ma is presented from Site 1124. These sediment parameters allow interpretations of DWBC velocities that indicate the establishment of the ACC to modern pathways and intensities at approximately 23 Ma, as the tectonic seaways expanded, completing the thermal isolation of Antarctica. The sediment parameters used in this study appear to be very sensitive to fluctuations of the Southwest Pacific DWBC between 23 and 9 Ma, and are in concordance with major Antarctic episodes of glacial development and circulation changes. The hiatus between 22.5 and 17.6 Ma represents an increase in thermohaline circulation around Antarctica due to the recent opening of circum-Antarctic gateways, while the hiatuses at 16.5–15 and 14–11 Ma represent glacial periods on Antarctica and major fluctuations in the East Antarctic Ice Sheet separated by periods of relative warmth. The time period from 11 to 9 Ma is characterized by conditions surrounding the formation and stabilization of the West Antarctic Ice Sheet.

The sediment record at Site 1124 from 9 Ma and younger contains a history of New Zealand climate and tectonics. The lack of indications of current activity during this time period is likely a local effect caused by the relative movement of the DWBC away from the 1124 location. Depositionally, it is not a sediment drift environment during this time.

The delivery of terrigenous sediment from New Zealand to the continental margin increases at approximately 10 Ma, and volcanic activity started during the late Miocene. The Hikurangi Channel shifted to its path across the Hikurangi Plateau to the continental margin during the Pliocene or Pleistocene. Despite all these potential sediment inputs, terrigenous MARs remain fairly low and constant through the Pleistocene.

Acknowledgements

We thank the Leg 181 scientific party, staff, and crew of the *JOIDES Resolution*, without which this paper would not have been possible; the information gained is certainly a group effort. Eun Park was of much assistance in the laboratory. We appreciate the helpful comments and thoughtful reviews provided by Lionel Carter, Ben Flower, Ted Moore, Josep Pares, and Don Zak. Ian Hall graciously provided the orbitally-tuned timescale for the youngest part of our record. Post-cruise funding was provided by JOI–USSAC. This research used samples and data provided by the Ocean Drilling Program (ODP). The ODP is sponsored by the U.S. National Science Foundation (NSF) and participating countries under management of Joint Oceanographic Institutions (JOI), Inc.

References

Bandy, O.L., Casey, R.E., Wright, R.C., 1971. Late Neogene planktonic zonation, magnetic reversals, and radiometric dates, Antarctic to the tropics, Antarctic oceanology, I. Antarct. Res. Ser. 15, 1–26.

Boven, K.L., Rea, D.K., 1998. Partitioning of eolian and hemipelagic sediment in eastern equatorial Pacific core TR 163–31B and the Late Quaternary paleoclimate of the northern Andes. J. Sediment. Res. 68, 850–855.

Broecker, W.S., 1997. Thermohaline circulation, the Achilles heel of our climate system: Will man-made CO_2 upset the balance? Science 278, 1582–1588.

Cande, S.C., Kent, D.V., 1995. Revised calibration of the geomagnetic polarity timescale for the Late Cretaceous and Cenozoic. J. Geophys. Res. 100, 6093–6095.

Carter, L., McCave, I.N., 1994. Development of sediment drifts approaching an active plate margin under the SW Pacific Deep Western Boundary Current. Paleoceanography 9, 1061–1085.

Carter, L., McCave, I.N., 1997. The sedimentary regime beneath the Deep Western Boundary Current inflow to the southwest Pacific Ocean. J. Sediment. Res. 67, 1005–1017.

Carter, L., Mitchell, J.S., 1987. Late Quaternary sediment pathways through the deep ocean, east of New Zealand. Paleoceanography 2, 409–422.

Carter, L., Shane, P., Alloway, B., Hall, I.R., Harris, S.E., Westgate, J.A., 2003. Demise of one volcanic zone and birth of another – A 12 m.y. marine record of major rhyolitic eruptions from New Zealand. Geology 31, 493–496.

Carter, L., Wilkin, J., 1999. Abyssal circulation around New Zealand – a comparison between observations and a global circulation model. Mar. Geol. 159, 221–239.

Carter, R.M., Carter, L., 1987. The Bounty Channel system: A 55-million-year-old sediment conduit to the deep sea, southwest Pacific Ocean. Geo-Mar. Lett. 7, 183–190.

Carter, R.M., Carter, L., McCave, I.N., 1996. Current controlled sediment deposition from the shelf to the deep ocean: The Cenozoic evolution of circulation through the SW Pacific gateway. Geol. Rundsch. 85, 438–451.

Carter, R.M., Landis, C.A., 1972. Correlative Oligocene unconformities in Southern Australia. Nature 237, 12–13.

Carter, R.M., McCave, I.N., Richter, C., et al., 1999. Proceedings of the Ocean Drilling Program, Initial Results, 181, 80.

Carter, R.M., Norris, R.J., 1976. Cainozoic history of southern New Zealand: An accord between geological observations and plate-tectonic predictions. Earth Planet. Sci. Lett. 31, 85–94.

Clemens, S.C., Prell, W.L., 1990. Late Pleistocene variability of Arabian Sea summer monsoon winds and continental aridity: Eolian records from the lithogenic component of deep-sea sediments. Paleoceanography 5, 109–145.

Exon, N.F., Kennett, J.P., Malone, M.J., et al., 2001. Proc. Ocean Drill. Prog., Init. Rep. 189 (available from the World Wide Web: 〈http://www-odp.tamu.edu/publications/189_IR/189ir.htm〉).

Flower, B.P., Kennett, J.P., 1993. Middle Miocene ocean/climate transition: High-resolution stable isotopic records from DSDP Site 588A, southwest Pacific. Paleoceanography 8, 811–843.

Flower, B.P., Kennett, J.P., 1994. The middle Miocene climatic transition: East Antarctic ice sheet development, deep ocean circulation and global carbon cycling. Palaeogeogr. Palaeoclimatol. Palaeoecol. 108, 537–555.

Flower, B.P., Kennett, J.P., 1995. Middle Miocene deepwater paleoceanography in the southwest Pacific: Relations with East Antarctic Ice Sheet development. Paleoceanography 10, 1095–1112.

Fulthorpe, C.S., Carter, R.M., Miller, K.G., Wilson, J., 1996. Marshall Paraconformity: A mid-Oligocene record of inception of the Antarctic Circumpolar Current and coeval glacio-eustatic lowland? Mar. Pet. Geol. 13, 61–77.

Hall, I.R., Carter, L., Harris, S.E., 2002. Major depositional events under the deep Pacific inflow. Geology 30, 487–490.

Hall, I.R., McCave, I.N., Schackleton, N.J., Weedon, G.P., Harris, S.E., 2001. Intensified deep Pacific inflow and ventilation in Pleistocene glacial times. Nature 412, 809–812.

Hall, I.R., McCave, I.N., Zahn, R., Carter, L., Knutz, P.C., Weedon, G.P., 2003. Paleocurrent reconstruction of the deep Pacific inflow during the middle Miocene: Reflections of East Antarctic Ice Sheet growth. Paleoceanography 18-1-11.

Haq, B.U., Hardenbol, J., Vail, P.R., 1987. Chronology of fluctuating sea levels since the Triassic. Science 235, 1156–1167.

Hovan, S.A., 1995. Late Cenozoic atmospheric circulation intensity and climatic history recorded by eolian deposition in the eastern Equatorial Pacific Ocean, Leg 138. Proc. Ocean Drill. Prog., Sci. Results 138, 615–625.

Joseph, L.H., 2001. Late Cretaceous through Cenozoic Climate Change on Antarctica: A View from the Deep Sea. Ph.D. Thesis, University of Michigan, Ann Arbor.

Joseph, L.H., Rea, D.K., van der Pluijm, B.A., 1998. Use of grain size and magnetic fabric analyses to distinguish among depositional environments. Paleoceangraphy 13, 491–501.

Joseph, L.H., Rea, D.K., van der Pluijm, B.A., 2002. Antarctic environmental variability since the late Miocene: ODP Site 745, the East Kerguelen sediment drift. Earth Planet. Sci. Lett. 201, 127–142.

Kamp, P.J.J., 1986. Late Cretaceous–Cenozoic tectonic development of the southwest Pacific region. Tectonophysics 121, 225–251.

Keller, G., Barron, J.A., 1983. Paleoceanographic implications of Miocene deep-sea hiatuses. Geol. Soc. Am. Bull. 94, 590–613.

Kemp, E.M., 1978. Tertiary climatic evolution and vegetation history in the southeast Indian Ocean region. Palaeogeogr. Palaeoclimatol. Palaeoecol. 24, 169–208.

Kennett, J.P., 1977. Cenozoic evolution of Antarctic glaciation, the circum-Antarctic Ocean, and their impact on global paleoceanography. J. Geophys. Res. 82, 3843–3860.

Kennett, J.P., 1980. Paleoceanographic and biogeographic evolution of the Southern Ocean during the Cenozoic, and Cenozoic microfossil datums. Palaeogeogr. Palaeoclimatol. Palaeoecol. 31, 123–152.

Kennett, J.P., 1995. A review of polar climatic evolution during the Neogene, based on the marine sediment record. In: Vrba, E., Denton, G., Partridge, T., Burckle, L. (Eds.), Paleoclimate and Evolution with Emphasis on Human Origins. Yale University Press, New Haven, pp. 49–64.

Kennett, J.P., Burns, R.E., Andrews, J.E., Churkin, M.J., Davies, T.A., Dumitrica, P., Edwards, A.R., Galehouse, J.S., Packham, G.H., van der Lingen, G.J., 1972. Australian–Antarctic continental drift, palaeocirculation changes and Oligocene deep-sea erosion. Nature 239, 51–55.

Kennett, J.P., Stott, L.D., 1990. Proteus and proto-oceanus: Ancestral paleogene oceans as revealed from Antarctic stable isotopic results; ODP Leg 113. Proc. Ocean Drill. Prog., Sci. Results 113, 865–880.

Kuijpers, A., 1989. Southern Ocean circulation and global climate in the Middle Pleistocene (early Bruhnes). Palaeogeogr. Palaeoclimatol. Palaeoecol. 79, 67–83.

Lawver, L.A., Gahagan, L.M., Coffin, M.F., 1992. The development of paleoseaways around Antarctica. Antarct. Res. Ser. 56, 7–30.

Lazarus, D., Caulet, J.P., 1993. Cenozoic Southern Ocean reconstructions from sedimentologic, radiolarian, and other microfossil data. Antarct. Res. Ser. 60, 145–174.

Lewis, K.B., Collot, J.-Y., Lallem, S.E., 1998. The dammed Hikurangi Trough: A channel-fed trench blocked by subducting seamounts and their wake avalaches. Basin Res. 10, 441–468.

McCave, I.N., Carter, L., 1997. Recent sedimentation beneath the Deep Western Boundary Current off northern New Zealand. Deep-Sea Res. I 44, 1203–1237.

Nye, J.F., 1957. Physical Properties of Crystals. Clarendon, Oxford, 322 pp.

Nye, J.F., 1985. Physical Properties of Crystals. Clarendon, Oxford, 329 pp.

Orsi, A.H., Johnson, G.C., Bullister, J.L., 1999. Circulation, mixing, and production of Antarctic Bottom Water. Prog. Oceanogr. 43, 55–109.

Orsi, A.H., Whitworth, T., III, Nowlin, W.D.J., 1995. On the meridional extent and fronts of the Antarctic Circumpolar Current. Deep-Sea Res. I 42, 641–673.

Rait, G., Chanier, F., Waters, D.W., 1991. Landward- and seaward-directed thrusting accompanying the onset of subduction beneath New Zealand. Geology 19, 230–233.

Rea, D.K., Hovan, S.A., 1995. Grain size distribution and depositional processes of the mineral component of abyssal sediments: Lessons from the North Pacific. Paleoceanography 10, 251–258.

Rea, D.K., Janecek, T.R., 1981. Mass-accumulation rates of the non-authigenic inorganic crystalline (eolian) component of deep-sea sediments from the western Mid-Pacific Mountains, Deep Sea Drilling Project Site 463. Init. Rep. Deep Sea Drill. Proj. 62, 653–659.

Schuur, C.L., Coffin, M.F., Frohlich, C., Massell, C.G., Karner, G.D., Ramsay, D., Caress, D.W., 1998. Sedimentary regimes at the Macquarie Ridge Complex: Interaction of Southern Ocean circulation and plate boundary bathymetry. Paleoceanography 13, 646–670.

Stickley, C.E., Carter, L., McCave, I.N., Weaver, P.P.E., 2001. Lower Circumpolar Deep Water flow through the SW Pacific Gateway for the last 190 ky: Evidence from Antarctic diatoms. In: Seidov, D., Haupt, B.J., Maslin, M. (Eds.), The Oceans and Rapid Climate Change, Geophysical Monograph 126, American Geophysical Union, Washington, DC, pp. 101–116.

Tarling, D.H., Hrouda, F., 1993. The Magnetic Anisotropy of Rocks. Chapman and Hall, New York, 217 pp.

Veevers, J.J., 2000. Change of tectono-stratigraphic regime in the Australian plate during the 99 Ma (mid Cretaceous) and 43 Ma (mid-Eocene) swerves of the Pacific. Geology 28, 47–50.

Walcott, R.I., 1978. Present tectonics and Late Cenozoic evolution of New Zealand. Geophys. J. R. Astron. Soc. 52, 137–164.

Warren, B.A., 1973. Transpacific hydrographic sections at Lats. 43°S and 28°S: The SCORPIO Expedition-II Deep water. Deep-Sea Res. 20, 9–38.

Webb, P.-N., Harwood, D.M., 1991. Late Cenozoic glacial history of the Ross Embayment, Antarctica. Quat. Sci. Rev. 10, 215–223.

Whitworth, T.I., Warren, B.A., Nowlin, W.D.J., Rutz, S.B., Pillsbury, R.D., Moore, M.I., 1999. On the deep western-boundary current in the Southwest Pacific Basin. Prog. Oceanogr. 43, 1–54.

Wright, J.D., Miller, K.G., 1993. Southern Ocean influences on late Eocene to Miocene deepwater circulation. Antarct. Res. Ser. 60, 1–35.

Zachos, J., Pagani, M., Sloan, L., Thomas, E., Billups, K., 2001. Trends, rhythms, and aberrations in global climate 65 Ma to present. Science 292, 686–693.